A FAST AND ROBUST METHOD FOR VOLUMETRIC MRI BRAIN EXTRACTION

Sami Bourouis and Kamel Hamrouni
Ecole Nationale d'Ingénieurs de Tunis
Laboratoire de Systèmes et de Traitement du Signal : LSTS
ENIT, BP-37, Le Belvédère 1002 Tunis, Tunisia

Keywords: Magnetic Resonance Imaging (MRI), 3D Segmentation, Brain extraction, Expectation Maximization, Level-set method.

Abstract: This paper presents a method for magnetic resonance imaging (MRI) segmentation and the extraction of main brain tissues. The method uses an image processing technique based on level-set approach and EM-algorithm. The paper describes the main features of the method, and presents experimental results with real volumetric images in order to evaluate the performance of the method.

1 INTRODUCTION

In brain imaging, image analysis such as segmentation of anatomical structures is a very important yet open research problem and is often a first step in the study of brain anatomy and function. In the context of neuro-imaging, 3D segmentation of white matter, gray matter, CSF, etc. is extremely important and has received much interest in the literature for the reconstruction, visualization, interpretation of the brain activity, and quantitative analysis such as volume measurements. On the other hand, Magnetic Resonance Imaging (MRI) has become of great interest in many research areas. This modality allows neuroscientists to see inside a living human brain, to better localize specific areas inside the brain and to understand the relationship between them. However, brain segmentation and especially the extraction of anatomical structures from MRI images are a complex problem, because medical images usually involve a large amount of data and they sometimes present various artefacts in the imaging process such as noise, partial volume effects, intensity inhomogeneities, and because of the highly convoluted nature of the brain cortex itself. Thus, it is very difficult to obtain a powerful segmentation tools to be used in clinical routine. This assertion is even more valid in the case of 3D segmentation of cerebral structures.

In the last several years, many algorithms have been proposed in this growing area, offering a diversity of methods and various evaluation criteria. For example, several general surveys are reported in (Pham et al., 1998; Sarang, 2000; Suri et al., 2002). Shattuck et al. (Shattuck et al., 2001) have developed a Brain Surface Extraction algorithm (BSE) based on statistical classification, mathematical morphology and connected component operations. In general, these methods work efficiently for some segmentation tasks, but partially fail for "hard cases". In addition, there is currently no segmentation method that provides acceptable results for every type of medical dataset. 3D brain segmentation using deformable model approach is an appropriate framework for merging heterogeneous information and provides a consistent geometrical representation suitable for a surface-based analysis. Deformable models are classified as either parametric active contours or geometric active contours according to their representation. Parametric active contours (snakes), originally proposed by Kass et al. (Kass et al., 1987), are represented explicitly as parameterized curves. However, their typical problem consists in its evolution and final results are depended on initial shape parameterization. Recently, several attempts have been made to apply geometric deformable models to brain image segmentation. In particular, Level-set method (Osher and Sethian, 1988) is becoming very popular thanks to its advantages over an explicit representation of the interface. Indeed, no parametrization is needed, topology changes are handled automatically, number

Bourouis S. and Hamrouni K. (2008).
A FAST AND ROBUST METHOD FOR VOLUMETRIC MRI BRAIN EXTRACTION.
In *Proceedings of the Third International Conference on Computer Vision Theory and Applications*, pages 461-466
DOI: 10.5220/0001078604610466

of dimensions is accommodated, and intrinsic geometric properties such as normal and curvature can be computed easily from the level set function. In addition, the level-set method has a sub-voxel precision in its segmentation, a property that very few segmentation methods provide. An interesting work on cortex segmentation using deformable models appears in (Davatzikos and Bryan, 1996) and (Sandor and Leahy, 1997). Also, Xu et al. (Xu et al., 1999) have presented a method for reconstructing cortical surfaces from MR brain images by combining fuzzy segmentation method, an isosurface algorithm, and a deformable surface model. In recent studies, several level set-based methods have been proposed. But, the problem is that most of these techniques require that the model should be initialized near the solution or supervised by an interactive interface. In addition, computational procedure is another limitation of using deformable level-set models.

The goal of this work is to provide an automatic segmentation, based on a level-set deformable model, for extracting accurately fronts from MR images. Also, we aim to outline the importance of reducing processing time in medical image analysis. Like several other recent approaches, our design is a successful combination of two approaches, which produces good results and requires less computing time. Here, unsupervised classification based on expectation-maximization (EM) and deformable level-set methods are integrated into the same pipeline. More precisely, we apply the EM algorithm and a connected component analysis on MRI scans to generate inputs to our deformable model. The synergy between different methodologies tends to result robustness and optimize processing time that several medical applications required them.

This paper is organized as follows. In Section II, we describe our proposed segmentation framework. In Section III, we present and discuss obtained results by our framework. Finally, in Section IV, we conclude our paper and point out future research directions.

2 SEGMENTATION BASED ON LEVEL-SET APPROACH

Automatic 3D segmentation of the brain from MR scans is a challenging problem that has received enormous amount of attention lately. Here, we present our automatic 3D segmentation procedure based on a deformable level-set method to extract accurately main tissues from MR images. We notice that a large number of computations are often needed to solve the variational equations involved in the Level-Set model. Nevertheless, good initialization could improve quality results. Furthermore, only few iterations are needed to converge to a sub-pixel accurate solution. For this reason, we plan to include prior information about the expected shape. Our proposition to overcome difficulties consists first on reducing initial data set to a smaller size. It is an important task in image analysis that allows overcoming the limitations of the processing time and become more and more important, especially, in the case of multidimensional signal processing. Thus, estimating parameters on the new sample can be done easily and rapidly.

Our brain extraction algorithm uses three stages to segment image. The first one is the dada smoothing and the all non-brain tissue removal (i.e. skin, bone, fat, etc.) from initial data set. In the second stage, we apply a downsampling process that reduces data size and furthermore overcomes computation time. The final stage consists of segmenting, with more precision, brain structures by using level-set method. Figure 1 illustrates the major computational steps in the proposed method.

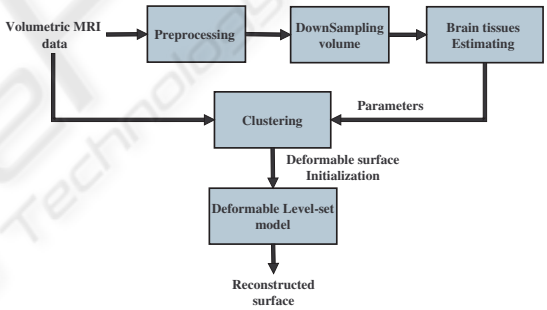

Figure 1: General principle of our method.

2.1 Preprocessing Data

Generally, the data volume can contain various amounts of noise. To eliminate noise, a smoothing filter is applied (Perona and Malik, 1990). This filter is supposed to remove only high-frequency noise and should not affect relevant major geometrical features. Authors formulate the anisotropic diffusion filter as diffusion process that encourages intra-region smoothing while inhibiting inter-region smoothing. The diffusion function is given as :

$$\frac{\partial I(\bar{X},t)}{dt} = \nabla(C(\bar{X},t).\nabla I(\bar{X},t)) \quad (1)$$

Where, $I(\bar{X},t)$ is the MR image. $\bar{X}$ refers to the image axes (i.e. x,y,z) and t refers to the iteration step. $C(\bar{X},t)$ is called the diffusion function and is a

monotonically decreasing function of the image gradient magnitude. It allows for locally adaptive diffusion strengths: edges are selectively smoothed or enhanced based on the evaluation of the diffusion function.

Figure 2 illustrates the effect of the anisotropic diffusion filter on MRI brain. In our case, the parameter time step was 0.125, the number of iterations was 5, and the conductance value was 3.0. In This result we show how the volume data is smoothed and edges are preserved.

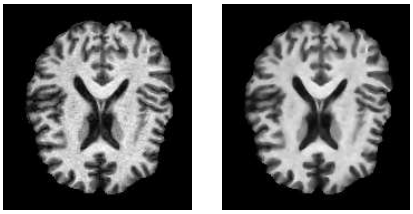

Figure 2: Effect of the anisotropic diffusion filter on an MRI brain image. (left) original data, (right) smoothed data.

2.2 Non-Brain Tissue Removal

Removal of non brain tissue from the MR volume can facilitates later stages in the algorithm as fewer voxels and fewer tissue types are involved. On the other hand, only brain tissue is retained and all non-brain tissues are masked out. A number of techniques have been proposed for brain mask extraction from MRI data. Here, we have applied the standard technique called -Brain Extraction Tool (BET)- which has been proposed by Smith et al. (Smith, 2002). This algorithm uses deformable model technique, which evolves to fit the brain's surface by the application of a set of locally adaptive model forces. It can remove skull, scalp, and other tissue from the MR image. An illustration of this process is shown in figure 3.

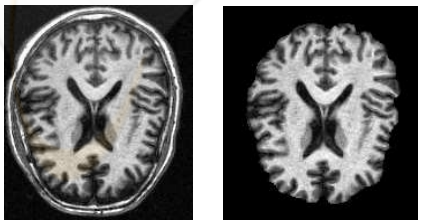

Figure 3: Removal of extracerebral tissues. (left) original image, (right) cerebral structures.

2.3 Downsampling Volume

In computer graphics, downsampling (or "resampling") is the process of reducing an image to a smaller size. Changing the pixel dimensions of an image is called also resampling. The downsampling process is an important task in image analysis that decreases computation time and improves rendering performance. Therefore, an improvement in speed could be gained by downsampling the initial volumetric data before any other processing. The gain in speed could be obtained by the reduction of the number of voxels. For example if the dimension of an input MRI volume is 256 x 256 x 150 voxels and if this MRI was downsampled from 1.0 mm^3 to (2.0 x 2.0 x 5) mm^3 in the x-, y- and z-directions respectively, then the output volume dimensions are 128 x 128 x 30 voxels. Therefore, downsampling the input volume of 9,830,400 voxels to an output volume of 491,520 voxels drops out 95% of the voxels from the input volume. Thus, next statistical estimation will be performed by the resampled data and level-set evolution will be done on original smoothed volume.

2.4 Estimation Maximization

The classification step is intended to provide an initial model that can be refined using level-set. In the case of unsupervised classification, the Expectation Maximization (EM) algorithm (Dempster et al., 1977), is an efficient iterative procedure to compute the Maximum Likelihood (ML) estimate in the presence of hidden data $\boldsymbol{f}$. In short, the EM algorithm alternates between two steps: an expectation (E) step and a maximization (M) step. In the E-step, the missing data are estimated given the observed data and current estimate of the model parameters. In the M-step, we compute the maximum likelihood estimates of the parameters by maximizing the expected likelihood found in the E-step. The parameters found in the M-step are then used to begin another E-step, and the process is repeated. The method classifies resampled image into white matter (WM), grey matter (GM) and cerebrospinal fluid (CSF).

Let us consider the mean parameter μ_k and the variance parameter σ_k of the intensity distribution of the k-th tissue class grouped in θ_k such as $\theta_k = \{\mu_k, \sigma_k\}$. We denote also π^k the prior probability of each class k and γ_i^k the posteriori probability calculated in each voxel $\boldsymbol{i}$ for each class k. In the expectation step, we calculate the posteriori probability according to the following formulas:

$$\gamma_i^k = P(x_k/y_k, \theta_k) = \frac{\pi_i^k f_k(y_i/\theta_k)}{\sum_{l=1}^{K} \pi_i^l f_l(y_i/\theta_l)} \qquad (2)$$

In the maximization step, we estimate data driven parameters by:

$$\begin{cases} \pi_k = \frac{\sum_{i=1}^{K} \gamma_i^k}{N} \\ \mu_k = \frac{\sum_{i=1}^{K} \gamma_i^k y_i}{\sum_{i=1}^{K} \gamma_i^k} \\ \sigma_k^2 = \frac{\sum_{i=1}^{K} \gamma_i^k (y_i - \mu_k)(y_i - \mu_k)}{\sum_{i=1}^{K} \gamma_i^k} \end{cases} \quad (3)$$

2.5 Clustering

Gaussian parameters obtained previously on the downsampled volume are generally identical to those obtained on whole volume. In this way, an improvement in speed could be gained in the clustering step. At this step, classification is restricted to three classes: gray matter (GM), white matter (WM) and CSF. Several classifiers could do this task such as k-means, Fuzzy k-means, k-NN, etc. However, we show that a simple clustering based on euclidian distance is sufficient. More precisely, each voxel is assigned to one class based on its minimum euclidian distance. This simple way decreases also computation time and provides good results. Figure 4 illustrates the effect of this clustering with three classes. The mean values are estimated by the EM algorithm.

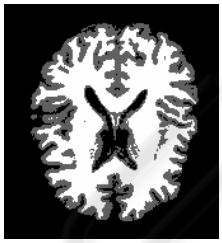

Figure 4: Clustering of the MR image (original image is shown in figure 3).

2.6 Level-set Method

The aim of this step is to extract accurately the boundary of the region-of-interest by using a deformable level-set model. Therefore, we exploit previous initialization to accelerate and to guide the process evolution. Level set method, initially introduced by Osher and Sethian (Osher and Sethian, 1988), has been used in many applications: physics, graphics, computer vision, image analysis, restoration, etc. It becomes also one of the popular frameworks for image segmentation. Theoretically, the level set function ψ will change with time according to the speed term $\boldsymbol{F}$ (as illustrated in the eq. 6) and the front Γ is always represented by the zero isosurface. ψ and Γ are defined as follows:

$$\psi : \begin{cases} \Omega \times [0, +\infty[\rightarrow IR \\ (x,y,t) \mapsto \psi(x,y,t) \\ \psi(x,y,t=0) = \pm d(x,\Gamma) \end{cases} \quad (4)$$

$$\Gamma(t) = \{(x,y) \in \Omega; \psi(x,y,t) = 0\} \quad (5)$$

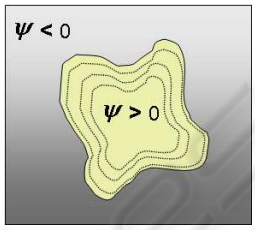

Figure 5: Level-set concept.

$\psi(t)$ takes opposite signs on each side of $\Gamma(t)$ (Fig.5). The evolution of $\psi(t)$ can be expressed as:

$$\frac{\partial \psi}{\partial t} = \boldsymbol{F}|\nabla\psi| = \alpha P(x)|\nabla\psi| + \beta k|\nabla\psi| \quad (6)$$

Where $\boldsymbol{P(x)}$ is a propagation (speed) term that controls surface expansion/contraction and $\boldsymbol{k}$ is a curvature term that controls the smoothness of the surface. α and β are scalar constants. The standard convention for level-set segmentation is that positive propagation term causes the surface to expand while negative term causes the surface to contract.

Different implementations of the level-set function are proposed in literature (Sethian, 1996). We notice that most of them are relatively sensitive to initial conditions. For best efficiency, the initial front should be the best guess possible for the solution. Here, we expect two inputs for our implementation. The first is an initial front, which is given by previous step (i.e. statistical classification), and the second is a feature image from which the propagation term $\boldsymbol{P(x)}$ is calculated (see eq. 4). In the feature image, values that are close to zero are associated with object boundaries and speed term is calculated as the laplacian of the image. The goal is to attract the evolving level set surface to local zero-crossings in the laplacian image. One nice property of using the laplacian is that there are no free parameters in the calculation and it is often used for edge detection. Finally, positive values in the output image are inside the segmented region and negative values are outside. The zero crossings of the image correspond to the position of the level set front.

2.7 3D Volume Rendering

Representing the surface as an explicit geometry is efficient when used with the conventional computer graphics approaches for shading and viewing. Further, it greatly reduces the necessary data storage and provides a data structure that can be measured. At this step, our segmentation is transformed into a triangulation using an isosurface "marching cubes" algorithm (Lorensen and Cline, 1987). More precisely, an isosurface is a surface that passes through all locations in space where a continuous data volume is equal to a constant value. However, the output triangulated surfaces usually contains multiple small "useless" meshes that are physically disconnected from each other. In order to reduce aliasing artefacts and produce a smooth surface estimation, we have applied the algorithm proposed by Whitaker (Whitaker, 2000).

3 EXPERIMENTAL RESULTS

At this stage, we have validated the performance of the proposed method on some 3D MRI data sets. Clustering process is limited to provide only three classes: GM, WM and CSF because our first objective is to prove speed and not to extract all internal tissues. In the first experiment, two different axial MRI data sets consisting of 181 slices have been tested. The voxel size is 1 mm^3. Figure 7 shows the final segmented white matter tissue.

Figure 6 shows the cpu time and the gaussian parameters obtained by our method. Processing was performed on a 1.5 Mhz Intel Pentium HP with 512 MB of RAM. The second column of the table presents different sample sizes of two initial data sets. The fourth column is reserved for the computation time. The three last columns illustrate mean values of the three classes (CSF, GM, WM) which are estimated by EM. According to these results, we notice that mean values of each class are almost the same ones to all samples and a notable gain in computation time was performed. However, the current process can provide poorer quality. For example, when we resample an image to larger pixel dimensions, the image will lose some detail and sharpness.

For instance, these first results are encouraging but further investigation is required to extend the algorithm to a large range of data.

3D MRI volume	Dimension of sampled volume	Voxel dimension	Time (seconds)	Parameter Estimating		
				μ1	μ2	μ3
MRI 1	181x217x181	1x1x1	3393.07	0.22	78.51	106.82
	64x64x181	3x3x1	370.52	0.24	78.44	106.85
	64x64x70	3x3x1	139.8	0.54	78.27	106.83
MRI 2	128x128x81	2x2x1	385.24	0.47	44.72	86.92
	81x81x81	2x2x1	161.66	0.87	44.59	86.85
	60x60x81	3x3x1	88.03	1.24	44.74	86.96
	81x81x40	2x2x2	84.54	0.99	44.62	86.91
	60x60x27	3x3x1	55.51	1.00	44.79	87.04
	60x60x40	3x3x1	42.82	1.44	44.77	87.03

Figure 6: CPU times (in seconds) and parameter estimation provided by our algorithm : application on two normal MR Data with different samples.

4 CONCLUSIONS

In this paper, we have proposed method for 3D MRI brain segmentation problem. We have explored the use of deformable level-set models to segment accurately different brain tissues. The algorithm gives satisfying results for brain tissues segmentation. It is also relatively computationally efficient and fast. At this stage, we have only presented preliminary results to demonstrate its potential: Even if they have not yet been compared to manual or other automatic segmentation results, we think that they are encouraging and faster than manual procedures.

However, clinical validation remains to be done, which will require additional work. Future validations will compare our segmentation with manually labelled data and other segmentation results. Future work could be the integration of anatomical knowl-

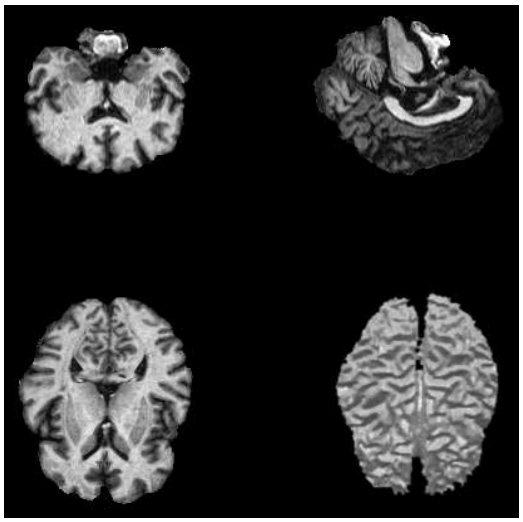

Figure 7: White matter segmented using our implementation.

edge to improve segmentation performance. Finally, the same framework can be used and extended to segment and quantify abnormal brains.

REFERENCES

Davatzikos, C. and Bryan, R. (1996). Using a deformable surface model to obtain a shape representation of the cortex. *IEEE Trans. Med. Imag*, 15:785–795.

Dempster, A., Laird, N., and Rubin, D. (1977). Maximum likelihood from in complete data via the em algorithm. *Journal of the Royal Statistical Society*, 1:1–38.

Kass, M., Witkin, A., and Terzopoulos, D. (1987). Snakes: Active contour models. *Int. J. Comput. Vis.*, 1:321–331.

Lorensen, W. and Cline, H. (1987). Marching cubes: A high-resolution 3-d surface construction algorithm. *ACM Comput. Graph*, 21:163–170.

Osher, S. and Sethian, J. (1988). Fronts propagating with curvature-dependent speed: Algorithms based on Hamilton-Jacobi formulations. *Journal of Computational Physics*, 79:12–49.

Perona, P. and Malik, J. (1990). Ieee transactions on pattern analysis machine intelligence. *IEEE Trans. Med. Imaging*, 12:629–639.

Pham, D., Xu, C., and Prince, J. (1998). A survey of current methods in medical image segmentation. *Technical report, Johns Hopkins University, Baltimore*.

Sandor, S. and Leahy, R. (1997). Surface-based labeling of cortical anatomy using a deformable atlas. *IEEE Trans. Med. Imaging*, 16:41–54.

Sarang, L. (2000). 3D segmentation techniques for medical volumes. *Technical report, State University of New York at Stony Brook*.

Sethian, J. (1996). Level set methods and fast marching methods. *Cambridge University Press*.

Shattuck, D., Leahy, S. S., Schaper, K., Rottenberg, D., and Leahy, R. (2001). Magnetic resonance image tissue classification using a partial volume model. *Neuroimage*, 13:856–876.

Smith, S. (2002). Robust automated brain extraction. *Human Brain Mapping*, 17:143–155.

Suri, J., Singh, S., and Reden, L. (2002). Computer vision and pattern recognition techniques for 2-d and 3-d mr cerebral cortical segmentation (part i): A state-of-the-art review. *Pattern Analysis and Applications*, 5:46–76.

Whitaker, R. (2000). Reducing aliasing artifacts in isosurfaces of binary volumes. *IEEE Volume Visualization and Graphics Symposium*, 21:23–32.

Xu, C., Pham, D., Rettmann, M., Yu, D., and Prince, J. (1999). Reconstruction of the human cerebral cortex from magnetic resonance images. *IEEE Transactions on Medical Imaging*, 18:467–480.